RESILIENT INFRASTRUCTURE
June 1–4, 2016

EXPERIMENTAL STUDY ON THE CAPACITY OF BARRIER DECK ANCHORAGE IN MTQ PL-3 BARRIER REINFORCED WITH HM-GFRP BARS WITH HEADED ENDS

Michael Rostami
Department of Civil Engineering, Ryerson University, Toronto, Ontario, Canada

Khaled Sennah
Department of Civil Engineering, Ryerson University, Toronto, Ontario, Canada

S. Milad Dehnadi
Department of Civil Engineering, Ryerson University, Toronto, Ontario, Canada

ABSTRACT

A recent design work conducted at Ryerson University on PL-3 bridge barrier has led to an economical glass fibre reinforced polymer (GFRP) bar detailing for sustainable construction. A PL-3 barrier wall of 27.6 m length was constructed using the proposed GFRP bar configuration, incorporating the use of V-Rod headed-end bars. The proposed barrier configuration was recently crash tested to qualify its use in Canada's highway bridges. Then, wall segments of this barrier were tested under static loading to-collapse to determine their structural behavior, crack pattern and ultimate load carrying capacity under simulated vehicle impact load. Test results led to establishing two Standard drawings by Ontario Ministry of Transportation (MTO) for use by consulting engineers and contractors. The crash-tested barrier dimensions were identical to those specified by Ministry of Transportation of Quebec (MTQ) for PL-3 barrier except that the base of the barrier was 40 mm short and the deck slab is of 200 mm thickness, leading to reduction in the GFRP embedment depth into the deck slab. As such, Ryerson University research team proposed an experimental program to ensure that the resistance of barrier-deck junction, with the reduced width of barrier base and thickness of the deck slab, is greater of equal to the specified factored design load applied to the barrier wall simulating vehicle impact. This paper summarizes the experimental program to justify the modified barrier design to fit with MTQ barrier and deck slab dimensions and experimental findings when compared to the available factored applied moments specified in CHBDC of 2006 for the design of barrier-deck junction. Correlation between the experimental findings and the factored applied moments from CHBDC equivalent vehicle impact forces resulting from the finite-element modelling of the barrier-deck system was conducted followed by recommendations for use of the proposed design in highway bridges in the Province of Quebec.

Keywords: Bridge barrier design, cantilever deck slab, truck impact, bridge code, experimental testing, FRP.

1. BACKGROUND OF RESEARCH

Until recently, the installation of GFRP bars was often hampered by the fact that bent bars have to be produced in the factory since GFRP bars cannot be bent at the site. Also, bent GFRP bars are much weaker than straight bars, due to the redirection and associated rearrangement of the fibres in the bend. As a result, number of bent GFRP bars is increased and even doubled at such locations where bar bents are required. The use of headed-end GFRP bars, shown in Fig. 1, is intended to eliminate the unnecessary and expensive use of custom made bar bends. The headed end is cast over the sand-coated bar as shown in Fig. 1. Recently, Ryerson University research team developed a cost-effective GFRP bar detailing for PL-3 barrier with MTO barrier dimensions. The GFRP bars used to develop reinforcement details, as shown in Fig. 2, were of sand-coated surface profile to ensure optimal bond between concrete and the bar. The 13M (#4) high-modulus (HM) GFRP bars of specified tensile strength of 1312 MPa, modulus of elasticity of 65.6 ± 2.5 GPa, and strain at rupture of 2%, as listed in the manufacturer's catalogue (Pultrall, 2013), were used as vertical bars at the back face of the barrier wall. Also, the 15M (#5) high-modulus

(HM) GFRP bars of specified tensile strength of 1184 MPa, modulus of elasticity of 62.5 ± 2.5 GPa, and strain at rupture of 1.89% were used in all other bars shapes shown in Fig. 2. The use of headed-end GFRP bars was proposed in this research to allow for anchorage in concrete at lower cost than the bend bars.

Fig. 1 View of HM-GFRP bar with end anchorage head

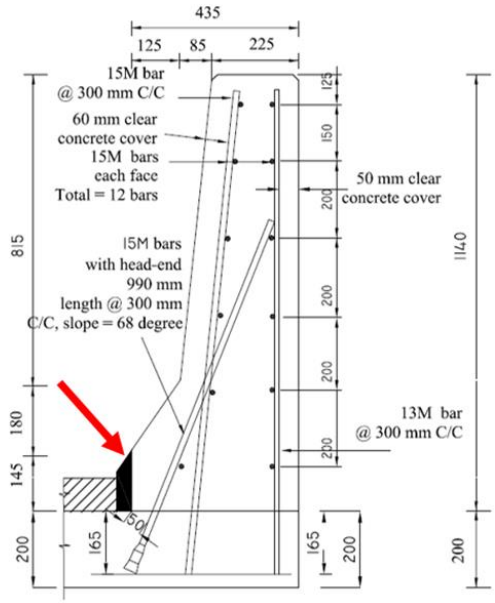

Fig. 2. Barrier cross-section showing the difference in geometry between the crash-tested MTO barrier and the proposed MTQ PL-3 barrier (the black-shaded area of 40 mm width is removed from the MTO crash-tested barrier dimension to reach MTQ barrier base width of 435 mm)

Recent research work conducted at Ryerson University on PL-3 bridge barrier proposed a cost-effective barrier configuration incorporating high-modulus GFRP bars with headed ends. To qualify the developed barrier configuration for use in bridge construction, a full-scale PL-3 barrier wall of 27.6-m length was constructed to perform vehicle crash testing in December 2011 (Sennah and Khederzadeh, 2014). The crash test was performed in accordance with MASH Test Level 5, TL-5, (MASH, 2009). Evaluation criteria for full-scale vehicle crash testing were based on three appraisal areas namely: (i) structural adequacy; (ii) occupant risk; and (iii) vehicle trajectory after collision. Results from the test qualified such innovative barrier system to resist vehicle impact per MASH crash test requirements. Crash test results showed that the developed barrier contained and redirected the vehicle. The vehicle did not penetrate, underride or override the parapet. No detached elements, fragments, or other debris from the barrier were present to penetrate or show potential for penetrating the occupant compartment, or to present undue hazard to others in the area. No occupant compartment deformation occurred. The test vehicle remained upright during and after the collision. After conducting the vehicle crash test on the developed GFRP-reinforced barrier shown in Fig. 2, full-scale static tests to-collapse were performed in other parts of this barrier at interior and exterior locations (Khederzadeh and Sennah, 2014) to investigate its ultimate load carrying capacity per Canadian Highway Bridge Design Code, CHBDC, (CSA, 2006a). The experimental ultimate load carrying capacity of the barriers was observed to be far greater than CHBDC factored design transverse load. The failure pattern was initiated by a trapezoidal crack pattern at the front face of the barrier, followed by punching shear failure at the transverse load location. Based on the punching shear failure developed in the barrier wall and comparison with available punching shear equations in the literature, an empirical punching shear equation was proposed to determine the transverse load carrying capacity of PL-3 bridge barrier walls reinforced with GFRP bars. To perform the above-mentioned static tests on the constructed barrier, Ryerson research team considered CHBDC provision that specifies transverse, longitudinal and vertical loads of 210, 70 and 90 kN, respectively, that can be applied simultaneously over a certain barrier length. CHBDC specifies that transverse load shall be applied over a barrier length of 2400 mm for PL-3 barriers. Since transverse loading creates the critical load carrying capacity, both the longitudinal and vertical loads were not considered in the design of barrier wall reinforcement and anchorages between the deck slab and the barrier wall. It should be noted that CHDBC specifies a live load factor of 1.7. Thus, the design equivalent impact load on PL-3 barrier wall over 2.4 m length is 357 kN.

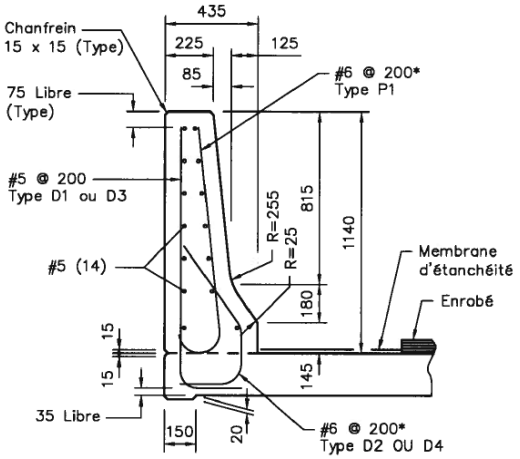

Fig. 3. Current dimensions and GFRP bar reinforcement for MTQ PL-3 tapered barrier (MTQ, 2013)

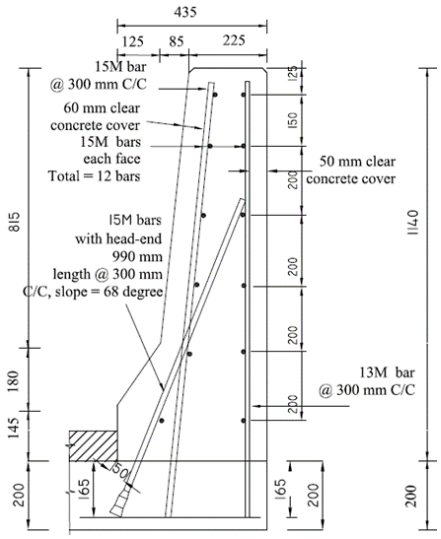

Fig. 4. View of the proposed MTQ PL-3 barrier with 200-mm thick deck slab,165 mm bar embedment in the deck and 435 mm base width

2. THE PROBLEM

Ministry of Transportation of Quebec (MTQ) specifies PL-3 barrier dimensions and GFRP bar detailing, shown in Fig. 3. By comparing MTQ barrier dimensions with those in the crash-tested barrier in Fig. 2, one may observe the difference in the width of barrier base at the barrier-deck junction (i.e. 475 mm in the crash-tested barrier and 435 mm in MTQ barrier). By drawing the two barriers in one graph as shown in Fig. 2, one may observe the black-shaded area, on the left side of the barrier-deck junction, of 40 mm width and about 117 mm deep, taken out from the crash-tested barrier to reach MTQ barrier dimension of 435 mm. Although the barrier base width decreased by about 8%, the diagonal headed bar at the lower tapered portion of the front face of the barrier becomes steeper by about 13% (i.e. with 68˚ slope in the MTQ barrier compared to 60˚ slope in the crash-tested barrier). It should be noted that increasing the slope of the diagonal GFRP bar from 60˚ to 68˚ increase the available vertical tensile force in the bar by 7% (i.e. sin 68 / sin60 = 1.07). On the other hand, MTQ requested that the concrete cover of the headed-end bar at the barrier-deck junction to be 50 mm as depicted in Fig. 4 in contrast to the 35 ± 10 mm concrete cover used the MTO crash-tested barrier details (Sennah and Khederzadeh, 2014). Since this change is at the barrier-deck junction, and the amount and shape of reinforcement as well as other barrier dimensions are identical to those in the crash-tested barrier, Ryerson research team believes that a static test in a constructed MTQ barrier segment in the laboratory would justify the change in the barrier width at the barrier-deck junction per CHBDC Clause 12.4.3.5. In addition, results on the static load tests on the crash-tested barrier (Khederzadeh and Sennah, 2014) resulted in a factor of safety in design in the order of 1.9 to prevent punching shear failure at the top of the barrier wall. Since the crash-tested barrier and MTQ barrier are of the same width, height and slope for the top tapered portion as well as the amount, type and arrangement of GFRP bars, one may observe similar behavior for punching shear capacity in the MTQ barrier. As for the thickness of the deck slab cantilever supporting the PL-3 barrier, the design of the crash-tested PL-3 barrier considered a minimum deck slab thickness of 225 mm, leading to a 195 mm vertical embedment length of the headed-end GFRP bars into the deck and a minimum concrete cover of 25 mm to the bottom surface of the deck slab cantilever. On the other hand, MTQ considers 200 mm thick slab with top and bottom reinforcement. To accommodate such change compared to the crash-tested barrier, Ryerson research team changed the embedment length of headed-end GFRP bar at the lower tapered portion of the front face of the crash-tested barrier shown in Fig. 2 to be 165 mm in the vertical direction for the proposed MTQ PL-3 barrier shown in Fig. 4. This allows for a concrete cover to the headed bar of 35 mm from the bottom surface of the 200-mm thick deck slab cantilever as shown in Fig. 4. As a result, the headed-end bar embedment length is proposed to change from 225 mm in the crash-tested barrier to 182 mm in the proposed MTQ barrier shown in Fig. 4. Also, the embedment length of the straight-end vertical bars at the back face of the barrier as well as the diagonal, straight-end, bars extending from the top tapered portion of the front face of the barrier changed from 185 mm in the crash-tested barrier to 165 mm in the proposed MTQ barrier. As mentioned earlier, the changes in bar anchorage in the

deck slab can be qualified by conducting static load testing in the laboratory for actual-size barrier of 900 mm length only. So, there is no need to repeat vehicle crash testing per CHBDC Clause 12.4.3.5. The objective of this research is to provide experimental data and numerical evaluation, using the finite-element modelling, as a proof of concept of, or to validate, the proposed changes to the GFRP bar anchorage at the barrier-deck junction to meet MTQ barrier dimensions compared to the crash-tested barrier-deck junction dimensions. The results from the experimental program on selected barrier segments are correlated to CHBDC factored applied moments at the barrier-deck junction specified in Table C5.4 of CHBDC Commentaries (CSA, 2006b) as well as the results from the finite-element computer modelling conducted by Ryerson research team.

3. EXPERIMENTAL PROGRAM

Three full-scale PL-3 barrier specimens of 900 mm length were erected and tested to-collapse to determine their ultimate load-carrying capacities and failure modes at deck barrier joint. Figure 5 shows schematic diagram of specimen S-1 that represent the interior segment of the proposed MTQ barrier. The barrier is reinforced with M15 GFRP vertical bars at the front face at 300 mm spacing and 13M GFRP vertical bars at the back face of the barrier wall at 300 mm spacing. All vertical GFRP bars are embedded into a 200-mm thick deck slab cantilever with vertical embedment length of 165 mm. The cantilever deck slab was reinforced in the main direction with M20 steel bars at 100 mm spacing. Specimen S-2 represent the exterior segment of the proposed MTQ barrier on which the vertical reinforcement at the front face of the barrier is doubled compared to those shown in Fig. 5 for specimen S-1. In this case, M15 GFRP vertical bars were used at the front face of the barrier at 150 mm spacing while the vertical reinforcement at the back face of the barrier is kept as M13 at 300 mm spacing. It should be noted that specimens S-1 and S-2 represent barrier construction in case of slab-on-girder bridge system.

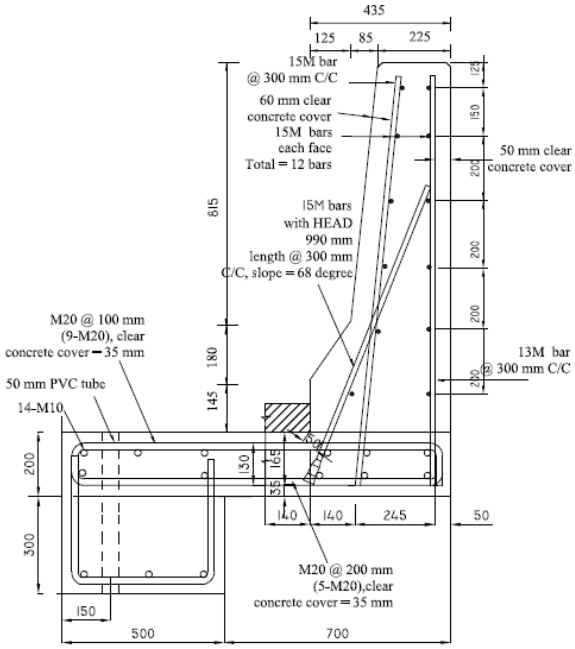

Fig. 5. Cross-section of specimens S-1 for interior portion of the barrier resting over deck slab cantilever

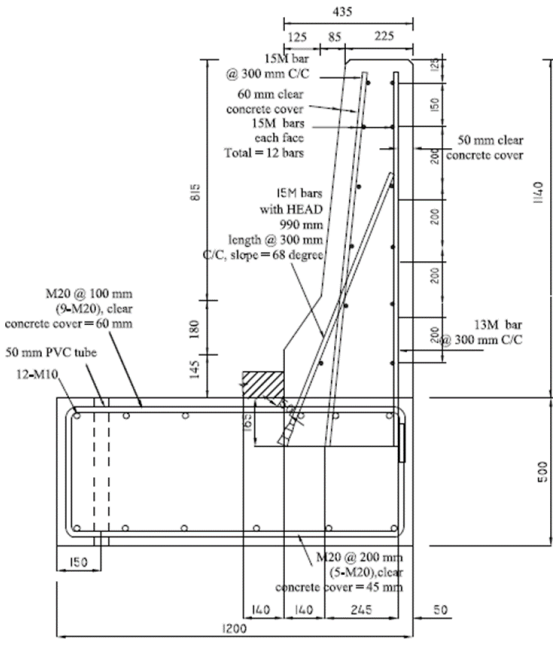

Fig. 6. Cross-section of specimens S-3 for interior portion of the barrier resting over thick deck slab

In case, barrier walls installed on top of solid slab bridges, voided slab bridges and adjacent box beam system, the barrier wall is considered connected to non-deformable thick slab compared to the case of barrier wall installed over 200-mm thick deck slab cantilever in slab-on-girder bridge system. Specimen S-3 shown in Fig. 6 represents this scenario where the barrier wall is fixed to a 500 mm thick slab resting on the laboratory floor to present its flexural deformation. The dimensions and GFRP arrangement are the same as those for specimen S-1. The embedment length of the barrier vertical GFRP bars into the thick solid slab base is maintained 165 mm. These three specimens represent the case of new construction. All specimens were cast using ready mix concrete with target compressive strength of 35 MPa. The test specimens were cast in the same day. In order to determine the strength of the concrete,

three 100×200 mm concrete cylinders collected from the concrete used to cast each barrier and then they batch were tested just after tested on the same day the barrier specimen were loaded to collapse. To take into account the effect of the number of tested cylinders and the deviation of the strength value of each cylinder with the average value, concrete characteristic strength was calculated using the available equation specified in CHBDC Chapter 14 for bridge evaluation (CSA, 2006a). Analysis of data resulted in the characteristic compressive strength of concrete as 39.72, 38.84 and 37.74 MPa for barrier specimens S-1, S-2 and S-3, respectively. Figure 7 shows the arrangement of GFRP and steel bars in the tested specimens. More information can be found elsewhere (Rostami, 2016). Figure 8 shows a schematic diagram of the test setup, while Fig. 9 shows view of specimen S-1 before testing. Each barrier specimen was supported over the structures laboratory floor, then, tied down to the floor using 50 mm diameter threaded rods. Each rod was placed @ 600 mm c-c and tightened by applying a specified torque to control the slab uplift during testing. A 900- kN hydraulic jack was used to apply horizontal load to the barrier wall. A universal flat load cell of 900 kN capacity was used to measure the applied loads on barrier models. SYSTEM 6000 data acquisition unit was used to record readings from all sensors. Each specimen was tested under increasing monotonic load up-to-collapse. During the test, jacking load was applied in increments 10 kN. At each load increment, the load was maintained for a few minutes to observe crack initiation and propagation as well as change in barrier geometry as depicted from potentiometer (POT) readings. Failure of the model was attained when the readings from sensors were increasing while the model did not take any further increase in load.

Specimen S-1 b) Specimen S-2 c) Specimen S-3

Fig. 7. View of internal reinforcement in the tested barrier specimens

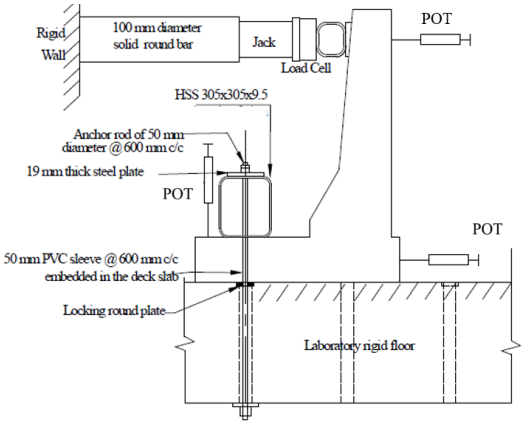

Fig. 8. Test setup showing the tie-down system for the deck

Fig. 9. View of the test setup for specimen S-1

4. EXPERIMENTAL RESULTS

4.1 Specimen S-1

Figure 9 shows the test setup of specimens S-1 before testing. While Fig. 10 shows different views of the crack pattern of the tested barrier specimen. In this specimen, the first visible crack was observed in the front side of the barrier wall at barrier-deck junction at 30 kN jacking load. Flexural cracks were observed in the deck slab at its fixed end and at the intersection of the tapered portion of the front side of the barrier wall at a jacking load of 60 kN.

These flexural cracks penetrated further at a higher load, along with other flexural cracks in the deck slab. Although flexural cracks appeared in the barrier wall and the deck slab portion, a sudden diagonal tension crack appeared in the deck slab at a jacking load of 80 kN on the right side of the barrier and at a jacking load of 86 kN at the left side of the barrier. These cracks propagated further till the barrier could not take a jacking load beyond 100.42 kN. Given the width of the barrier of 900 mm and the height of the applied load over the top surface of the deck slab of 990 mm, the experimental resisting moment is calculated as 110.46 kN.m/m. This experimental resisting moment at the barrier deck junction is greater than the CHBDC design value of 83 kN.m/m at the barrier-deck slab junction per Table 1 in this report. This leads to a factor of safety of 1.33 in the design of the proposed MTQ barrier wall at interior location as listed in Table 1

Table 1. Comparison of experimental failure load and CHBDC factored design moments at barrier-deck junction

	S-1	S-2	S-3
	Interior portion with cantilever slab and 300 mm bar spacing	Exterior portion with cantilever slab and 150 mm bar spacing	Interior with non-deformable solid slab and 300 mm bar spacing
Experimental failure load, kN	100.42	131.83	117.02
Experimental failure load, kN/m	111.58	146.48	130.02
Experimental resisting moment, kN.m/m	110.46	145.02	128.72
CHBDC-2006 design moment, kN.m/m	83.00	102.00	83.00
Factor of safety in design (experimental failure moment/ CHBDC-2006 design moment)	**1.33**	**1.42**	**1.55**

a) Crack pattern at the right side of the specimen b) Crack pattern at the left side of the specimen

Fig. 10.Views of crack pattern for specimen S-1 after failure

4.2 Specimen S-2

Specimen S-2 is identical to S-1 except that the vertical bars at the front face of the barrier wall are doubled to represent the exterior location of the barrier wall. Figure 11 shows different views of the crack pattern of the tested barrier specimen. In this specimen, the first visible crack was observed in the front side of the barrier wall at barrier-deck junction at 30 kN jacking load. Flexural cracks were observed in the deck slab at jacking load of 30 kN with other flexural cracks appeared at higher loads. Also, flexural crack appeared at the intersection of the tapered portion of the front side of the barrier wall at a jacking load of 80 kN. These flexural crack penetrated further into the barrier thickness at a higher load. Flexural cracks propagated into the barrier thickness at the barrier-deck junction with increase in applied load. However, a sudden diagonal tension crack appeared in the deck slab under the barrier wall at a load of 90 kN on the left side of the barrier wall and at a load of 100 kN at the right side of the barrier wall as depicted in Fig. 11. The recorded data in the data acquisition system showed that the barrier could not carry a jacking load beyond 131.83 kN. Given the width of the barrier of 900 mm and the height of the applied load over the top surface of the deck slab of 990 mm, the experimental resisting moment is calculated as 145.02 kN.m/m. This experimental resisting moment at the barrier deck junction is greater than the CHBDC design value of 102 kN.m/m

at the barrier-deck slab junction per Table 1 in this report. This leads to a factor of safety of 1.42 in the design of the proposed MTQ barrier wall at exterior location as listed in Table 1.

a) Crack pattern at the left side of the specimen

b) Crack pattern at the right side of the specimen

Fig. 11. Views of crack pattern for specimen S-2 after failure

4.3 Specimen S-3

Specimen S-3 represents a barrier connected to non-deformable concrete slab. The amount of vertical reinforcement at the front face represents the case of interior segment of the barrier wall. Figure 12 shows different views of the crack pattern of the tested barrier specimen. In this specimen, the first visible crack was observed in the front side of the barrier wall at barrier-deck junction at 60 kN jacking load. This observation coincide with the jacking load of about 60 kN at the end of the lower straight line portion of the load-deflection relationship for S-3. Flexural crack appeared at the intersection of the tapered portion of the front side of the barrier wall at a jacking load of 50 kN. Although flexural cracks at the barrier-deck junction penetrated further into the barrier thickness at a higher load, sudden concrete breakout appeared approximately at the embedded GFRP bar headed end at a load of 102 kN in each side of the barrier wall. These concrete breakout cracks extended towards the top surface of the solid slab and towards the back face of the barrier wall at higher loads till the barrier could not absorb jacking load beyond 117.02 kN. Given the width of the barrier of 900 mm and the height of the applied load over the top surface of the deck slab of 990 mm, the experimental resisting moment is calculated as 128.72 kN.m/m. This experimental resisting moment at the barrier deck junction is greater than the CHBDC design value of 83 kN.m/m at the barrier-deck slab junction per Table 1 in this report. This leads to a factor of safety of 1.55 in the design of the proposed MTQ barrier wall at interior location when it is rigidly connected to non-deformable concrete deck slab as listed in Table 1.

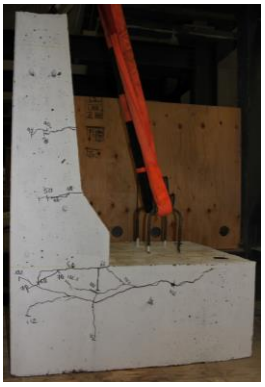

a) View crack pattern at left side of specimen

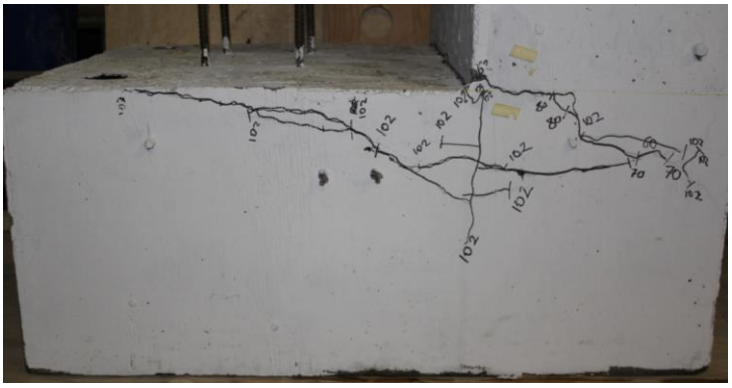

b) Close-up view of crack pattern at the right side of specimen

Fig. 12. Views of crack pattern for specimen S-3 after failure

5. LIMITATION OF USE OF CHBDC DESIGN TABLE FOR FACTORED APPLIED MOMENTS AT THE BARRIER-DECK JUNCTION

When an errant vehicle collides with the concrete bridge barrier, the effect of the lateral impact force is distributed in the barrier and the deck with dispersal angles shown in Fig. 13. This led to the design forces specified in CHBDC commentaries (CSA, 2006b). These forces were obtained by finite-element analysis as stated in the literature, assuming bridge cantilever of 1 m length. However, the bridge deck slab cantilever may be of different length which is the case of slab-on-girder bridges or the barrier wall can be rigidly fixed to a non-deformable base which is the case of thick solid slab bridges, voided slab bridges and adjacent box beam bridge system. As such, the change in the support system of the barrier wall should be investigated to ensure that it is properly addressed in the values of the design factored applied moments at the barrier-deck junction due to equivalent vehicle impact force. The design forces specified in CHBDC commentaries (CSA, 2006b) comprise moment and tension forces for the inner and end portions of the barrier. However, the Table does provide any further information for designers to obtain appropriate design moments and tensile forces for different barrier lengths and slab thicknesses. The length of a barrier is considered between two free ends of the barrier or between expansion joints. The length of the barrier will affect the dispersion angle of applied forces shown in Fig. 13. As such, finite-element computer modelling should be conducted to examine the effect of barrier length and the change in deck slab thickness on the factored applied moment at the barrier-deck junction.

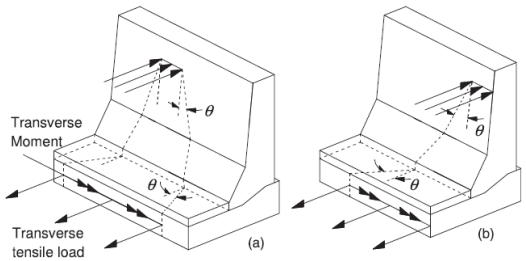

Fig. 13. Transverse load dispersion at (a) interior portion and (b) end portion of barrier wall

6. PARAMETRIC STUDY, USING FINITE-ELEMENT COMPUTER MODELLING, ON BARRIER-DECK ANCHORAGE MOMENTS

A parametric study was conducted to investigate the effect of key parameters on the barrier-deck anchorage forces. The design forces considered in this study were bending moment and tension force at the inner and end portions of the barrier shown in Fig. 13. The studied parameters include the deck slab thickness, t_s, cantilever overhang length, L_c, and the barrier length, L_b. The associated values for each parameter were taken as 175, 225, 275 and 350 mm for t_s; 0, 0.5, 1.0, 1.5, and 2.0 m for L_c; and 3, 4, 6, 8, 10, and 12 m for L_b. Finite-element (FEA) models were created for the PL-3 barrier with tapered face. The general purpose SAP2000 software was used to construct three-dimensional (3D) FE models to conduct linear elastic analysis of concrete barrier. The barrier wall and the deck slab were modeled using shell elements with six degrees of freedom at each node. The cantilever length, L_c, of 0 represents a fixed base of the barrier wall, simulating non-deformable deck slab. This is the case when the rigidity of the deck slab is significantly higher than that of the barrier wall. In addition, the minimum barrier length, L_b, is usually considered as 3m in practice. The maximum barrier length of 12 m was taken into consideration in this study because analysis showed that greater lengths would have insignificant effect on the distribution of forces in the inner portions of the barriers and no effect at the end portions of the barrier. On each barrier-deck FEA model, the lateral loads representing vehicle impact loading were placed at the middle of barrier for inner portion and at the end of barrier for the end portion. These forces were distributed over specified lengths at the given heights per CHBDC. Then, the resultant forces (i.e., moment and tension force) were obtained at the bottom of the barrier for a unit length parallel to lateral load. For inner portion, the unit length was considered at the centerline of the applied load, whereas for the end portion, the unit length was considered at the end of barrier. The results of this FEA analysis were presented elsewhere (Azimi et al., 2014). Representative results of the developed equations for applied factored moment at the barrier-deck junction obtained from FEA are shown in Table 2 for PL-3 barrier considered in this paper. By correlating data obtained from FEA modeling with those specified in CHBDC of 2006, it can be observed that CHBDC factored design moments are generally conservative for many case of cantilever lengths and slab thicknesses, whereas CHBDC underestimates these values in other cases. This can be attributed to the fact that

CHBDC equations were conducted using a FEA barrier model with deck slab cantilever of 1 m length and a certain slab thickness that is not mentioned in the literature. However, the current study showed that both slab thickness and cantilever length have significant effect on applied factored moment at the barrier-deck junction, especially for shorter barriers.

Table 2. Developed formulas for factored design moments at the barrier wall-deck interface (Azimi et al., 2014)

M_{inner} (kN.m)	Fixed base	132
	Cantilever deck slab	$100(L_b + 2.3t_s)^{-1} + 2.83t_s^{0.2}(L_b - 1)^{0.7} L_c^{-0.8} + 143t_s + 23$
M_{end} (kN.m)	Fixed base	148
	Cantilever deck slab	$14t_s^{-1}(L_b + 2.3t_s - 2)^{-1} + 2.83t_s^{0.2}(L_b - 1)^{0.7} L_c^{-0.7} + 240t_s + 25$

Notes: Formulas are best applicable for: $175mm \le t_s \le 350mm$; $0 \le L_c \le 2.0m$; $3.0m \le L_b$

t_s = overhang thickness (m); L_c = cantilever length (m) ; L_b = barrier length (m)

M_{inner} = moment in the inner portion of barrier; M_{end} = moment in the end portion of Barrier.

When applying the developed equations in Table 2 to the studied specimen S-3, it can be observed that the factor of safety in design (FOS) for the proposed barrier over non-deformable base is 0.98 compared to 1.55 obtained based on CHBDC-specified factored applied moment shown in Table 1. As such, it is recommended to increase the embedment length of the GFRP bars of the barrier wall resting over non-deformable deck slab from 165 mm to 195 mm. Results from FEA modelling and resulting equations in Table 2 showed that the FOS for the proposed barrier wall installed over deck slab cantilever increases with increase in deck slab cantilever length, for a given barrier length. Also, it can be observed that the FOS increases with increase of barrier length up to about 6 m, beyond which the increase in FOS is insignificant (Azimi et al., 2014). It should be noted that for barrier lengths equal of greater than 6 m, the FOS ranges from 1.41 to 1.63 with increase in barrier length up to 12 m, compared to a FOS of 1.33, shown in Table 1 based on the available CHBDC design factored moment for specimen S-1. Given the fact that the barrier length should be long enough to promote two-way action of truck impact load distribution, it is recommended to use the proposed GFRP-reinforced barrier resting over deck slab cantilever, shown in Fig. 4 for barrier length greater than or equal 6 m. This conclusion is also applicable to the barrier wall exterior location given the fact that for barrier lengths equal of greater than 6 m, the FOS for exterior location ranges from 1.41 to 1.64 with increase in barrier length up to 12 m, compared to a FOS of 1.42, shown in Table 1 based on the available CHBDC design factored moment.

7. CONCLUSIONS

Based on the data generated from the experimental program and the finite-element modelling, it is recommended to use the proposed MTQ GFRP-reinforced barrier system resting over 200-mm thick deck slab cantilever, shown in Fig. 4, for barrier length greater than or equal 6 m. This design is acceptable for slab-on-girder bridges as well as multiple-spine bridges with deck slab thickness of 200 mm and cantilever length ranging from 0.5 to 2 m. It is also recommended to use the proposed MTQ GFRP-reinforced barrier system shown in Fig. 4 in bridges with non-deformable deck slab provided that the embedment length of the GFRP bars into the non-deformable deck slab increases from 165 mm to 195 mm. Given the dimensions of the non-deformable concrete base supporting the barrier wall during tests, the proposed design is acceptable for applications in solid-slab and voided-slab bridge cross-sections with minimum deck thickness of 500 mm.

ACKNOWLEDGEMENTS

The authors acknowledges the support to this project by Pultrall Inc. of Quebec, Canada. The continuous support, commitment and dedication of Mr. Nidal Jaalouk, the senior technical officer of Ryerson University, were an integral part of the experimental work reported in this study.

REFERENCES

Azimi, H., Sennah, K., Tropynina, E., Goremykin, S., Lucic, S., and Lam, M. 2014. Anchorage Capacity of Concrete Bridge Barriers Reinforced with GFRP Bars with Headed Ends. ASCE Journal of Bridge Engineering, 19(9): 04014030 (1-15).

CSA. 2006a. Canadian Highway Bridge Design Code. CAN/CSA-S6-06. Canadian Standard Association, Toronto, Ontario, Canada.

CSA. 2006b. Commentary on CAN/CSA-S6-06, Canadian Highway Bridge Design Code. Canadian Standard Association, Toronto, Ontario, Canada.

Khederzadeh, H., and Sennah, K. 2014. Development of Cost-Effective PL-3 Concrete Bridge Barrier Reinforced with Sand-Coated GFRP Bars: Static Load Tests. Canadian Journal for Civil Engineering, 41(4): 368-379.

MASH. 2009. Manual for Assessing Safety Hardware, MASH. American Association of State Highway and Transportation Officials, Washington. D.C. 276 pages.

MTQ. 2009. Manuel de conception des structures, Chapter 16. Ministry of Transportation of Quebec.

Pultrall. 2013. V-Rod HM Data Sheet. Pultrall Inc. Quebec.

Rostami, M. Development of GFRP-reinforced bridge barrier deck-slab system for sustainable construction. Ph.D. Dissertation (expected December 2016), Civil Engineering Department, Ryerson University, Toronto, Ontario.

Sennah, K., and Khederzadeh, H. 2014. Development of Cost-Effective PL-3 Concrete Bridge Barrier Reinforced with Sand-Coated GFRP Bars: Vehicle Crash Test. Canadian Journal for Civil Engineering, 2014, 41(4): 357-367.